A Seed Placement Strategy for Conforming Voronoi Meshing

Ahmed Abdelkader* Chandrajit L. Bajaj† Mohamed S. Ebeida‡ Scott A. Mitchell§

Abstract

We show how to place a set of seed points such that a given piecewise linear complex is the union of some faces in the resulting Voronoi diagram. The seeds are placed on sufficiently small spheres centered at input vertices and are arranged into little circles around each half-edge where every seed is mirrored across the associated triangle. The Voronoi faces common to the seeds of such arrangements yield a mesh conforming to the input complex. If the input contains sharp angles, then additional seeds are needed, analogous to nonobtuse refinement. Finally, we propose local optimizations to reduce the number of seeds and output facets.

1 Introduction

In many applications, it is required to capture the geometry of some domain of interest, e.g., for the purposes of engineering design and simulations. When the input is a sufficiently dense sample of points from the boundary, surface reconstruction algorithms can produce a good approximation of the surface [1]. On the other hand, volume decompositions with theoretical guarantees can be obtained using tetrahedral cells. However, there has been a growing interest in polyhedral cells, which are known to be more efficient at filling the space with fewer cells and can offer certain advantages in terms of numerical stability. Utilizing the Voronoi cells of some interior sample of points has been considered, but ensuring that cells conform naturally to the surface, i.e., without clipping, remains challenging [6]. Similar to the study of conforming tetrahedral meshing [7, 8, 5], we study the analogous question in the polyhedral case. For background and applications of representing and approximating geometries by Voronoi cells, we refer the reader to [3, 9] and the references therein.

Given a piecewise linear complex (PLC) $\mathcal{C}$, we seek a reconstruction of $\mathcal{C}$, or rather a refinement of it, by Voronoi faces such that each input face is the union of a number of output faces. Depending on the geometry of $\mathcal{C}$, the number of Voronoi cells may be large, so those results are mostly of theoretical interest.

*University of Maryland, College Park, akader@cs.umd.edu
†University of Texas, Austin, bajaj@ices.utexas.edu
‡Sandia National Laboratories, msebeid@sandia.gov
§Sandia National Laboratories, samitch@sandia.gov

In Section 2, we show how to obtain a Voronoi mesh conforming to an input PLC. We rely on certain spherical neighborhoods being empty and assume we can place seeds arbitrarily close to input vertices. In Section 3, we show that seeds can be placed at a non-zero distance from vertices and that allowing overlapping sphere neighborhoods can help reduce the number of seeds needed. Finally, in Section 4, we describe refinement procedures to enforce the required empty neighborhood condition.

2 Basic Seed Placement Strategy

Allowing the seeds $\mathcal{S}$ to be placed arbitrarily close to features of $\mathcal{C}$, we develop the basis of the proposed strategy in 2.1. Then, sufficient conditions for such a strategy to work are derived in 2.2. We prove in 2.3 that a subset of $\mathrm{Vor}(\mathcal{S})$ yields a mesh that conforms to $\mathcal{C}$.

2.1 Overview

We place seeds near input faces, cospherical around vertices, cocircular around edges, and mirrored across triangles. We examine face types in sequence and anticipate sufficient conditions for correctness.

2.1.1 Placement for Vertices

A vertex v in $\mathrm{Vor}(\mathcal{S})$ is equidistant to at least four seeds in $\mathcal{S}$ which are closest to it, and are not cocircular. To ensure every vertex $v_i \in \mathcal{C}$ is a vertex in $\mathrm{Vor}(\mathcal{S})$, we define a sphere S_i of radius ϵ_v centered at v_i, and place at least four seeds on it. Using a sufficiently small ϵ_v, no other seeds lie inside S_i.

2.1.2 Placement for Edges

All points in the interior of an edge e in $\mathrm{Vor}(\mathcal{S})$ are equidistant to at least three seeds in $\mathcal{S}$, forming a circle perpendicular to and centered at the line supporting e. Each $e_{ij} = (v_i, v_j) \in \mathcal{C}$ can be reconstructed as two edges in $Vor(\mathcal{S})$. Define two circles C_{ij} and C_{ji} of radius ϵ_e on spheres S_i and S_j, perpendicular to and centered at e_{ij}. Three or more seeds on each circle are used to reconstruct the edge. For sufficiently small ϵ_v and ϵ_e, no other seeds on S_i or S_j are closer. Additional conditions, e.g., angle bounds, are required to ensure that no other seed is closer to any point on e_{ij}.

2.1.3 Placement for Triangles

All points in the interior of a Voronoi facet f are equidistant to the two seeds closest to f, such that the plane supporting the facet is the bisector between these seeds. For each triangle $\triangle_{ijk} \in \mathcal{C}$, each edge circle provides one mirrored pair of seeds at height h above and below $\triangle_{ijk}$. The value of h depends on the dihedral angle at the edge and is chosen to ensure that the seed pairs from the two adjacent triangles do not overlap. Additional conditions, e.g., obtuse dihedral angles, help ensure that no other seed is closer to any point on $\triangle_{ijk}$.

2.1.4 Recovering the PLC

For a vertex v_i with fewer than two edges, add extra seeds on S_i so there are at least four. All seeds on S_i get a *vertex label* ℓ_i^v. Circle C_{ij} contributes one pair of seeds for each triangle incident on e_{ij}; for edges with fewer than two triangles, add extra cocircular seeds so there are at least three. All seeds on C_{ij} get an *edge label* ℓ_{ij}^e. Finally, all seeds mirrored across facet $\triangle_{ijk}$ get a *facet label* ℓ_{ijk}^f. A labeled seed *witnesses* the associated input face. Denote the witnesses of face f by $\mathcal{S}_f$.

The refinement of $\mathcal{C}$ is the *witnessed* faces of $\mathrm{Vor}(\mathcal{S})$ shared between the appropriate number of seeds with matching labels. Denote these faces as $\mathrm{VoRef}(\mathcal{C}) \subset \mathrm{Vor}(\mathcal{S})$, where "subset" is as a complex. By construction, $\mathcal{S}_f$ refines f, $\forall f \in \mathcal{C}$. In Section 4, we show that non-manifold PLCs can be recovered using a more aggressive strategy requiring *extra* seeds.

2.2 Definitions and Preliminaries

Denote the input complex by $\mathcal{C} = (\mathcal{V}, \mathcal{E}, \mathcal{F})$, where $\mathcal{V}$ is a set of vertices in $\mathbb{R}^3$, $\mathcal{E}$ a set of edges and $\mathcal{F}$ a set of triangles. Note that $\mathcal{C}$ may contain *isolated vertices* not incident on any edges and *isolated edges* not incident on any triangles.

For $x \in \mathbb{R}^3$, let $N_0(x)$ be the closest points in $\mathcal{V}$ to x. Define $\kappa_0(x) := \|x - v\|$, with $v \in N_0(x)$, and let S_x be the sphere centered at x with radius $\kappa_0(x)$. Similarly, define $N(.)$ using $\mathcal{S}$, and $N_f(.)$ and $\kappa_f(.)$ using $\mathcal{S}_f$.

For edge e_{ij}, let m_{ij} be the midpoint and S_{ij} the *diametric-sphere*, i.e., the sphere with e_{ij} as a diameter. For $\triangle_{ijk}$, let S_{ijk} be the smallest enclosing sphere and c_{ijk} its center. Let (a, b) denote $\overline{ab} \setminus \{a, b\}$.

The basic strategy described in 2.1 requires the input to satisfy a condition like the following:

Definition 1 (Closeness) *$\forall x \in e_{ij}, N_0(x) \subseteq \{v_i, v_j\}$ if e_{ij} is isolated, and $\forall x \in \triangle_{ijk}$, $N_0(x) \subseteq \{v_i, v_j, v_k\}$.*

In 2.3, we prove that the basic strategy described in 2.1 can refine PLCs satisfying closeness. We use the following definition to characterize vertices close enough to spoil the closeness condition.

Definition 2 (ball neighborhood) *For an edge e_{ij} it is the diametric-sphere S_{ij}, and for a triangle $\triangle_{ijk}$ the union of the smallest enclosing S_{ijk} with $\{S_{ij}, S_{jk}, S_{ik}\}$.*

Lemma 3 *$\triangle_{ijk}$ has an empty ball neighborhood iff $\triangle_{ijk}$ satisfies the closeness condition.*

Proof. ($\Rightarrow$) WLOG take $x \in \triangle_{ijk}$ such that v_i is the nearest vertex in $\triangle_{ijk}$ to x. Letting S_p^i be the sphere centered at p with radius $\|v_i - p\|$, it is clear that if S_x^i is empty, $N_0(x) = v_i$ and closeness holds. Take $y = \overrightarrow{v_i x} \cap \overline{c_{ijk} m_{ij}}$ and observe that $S_x^i \subset S_y^i$. Let C_{ij} be the circle $S_{ijk} \cap S_{ij}$ centered at m_{ij}. For any $z \in C_{ij}$ we may write $\|m_{ij} - z\| = \|m_{ij} - v_i\|$. As $C_{ij} \perp \triangle_{ijk}$, $\overline{y m_{ij}} \perp \overline{m_{ij} z}$ and we get $\|y - z\|^2 = \|m_{ij} - z\|^2 + \|y - m_{ij}\|^2 = \|v_i - m_{ij}\|^2 + \|y - m_{ij}\|^2 = \|v_i - y\|^2$. Hence, $z \subset S_y^i$ implying $C_{ij} \subset S_y^i$. Recalling that $y \in \overline{c_{ijk} m_{ij}}$ we get $S_x^i \subset S_y^i \subset S_{ijk} \cup S_{ij}$, which is empty by assumption.

($\Leftarrow$) If $\exists v_a \in \mathcal{C}$ such that $v_a \in S_{ijk} \cup S_{ij}$ and $a \notin \{i, j, k\}$ then, either $v_a \in N_0(m_{ij})$ or $v_a \in N_0(c_{ijk})$. □

At first glance, empty ball neighborhoods appear rather restrictive. However, for planar triangulations, nonobtuseness is sufficient to guarantee it, which can be enforced by nonobtuse refinement [4].

For non-planar triangulations, nonobtuseness is not sufficient, and we must also consider the distance to non-incident vertices. We start in Section 4.1 by showing that for many common triangulations, empty ball neighborhoods can be guaranteed without much refinement. Then, in Section 4.2 we proceed to outline a more aggressive variant of the strategy, reminiscent of nonobtuse refinement [4], that ensures correct output regardless of input angles and distances. Hence, any PLC can be refined.

2.3 Placement under Closeness with $\epsilon_v \to 0$

We analyze the basic strategy in 2.1 for refining an input PLC $\mathcal{C}$ when the closeness condition (Definition 1) is satisfied. Throughout this analysis, we take $\epsilon_v, \epsilon_e \to 0$. Figure 1, illustrates the different ways in which the seeds in $\mathcal{S}$ refine a nonobtuse triangle. In 3.1, we show it is feasible for non-zero radii $\epsilon_v, \epsilon_e > 0$ within a constant factor of the smallest geometric distances and angle sines.

Claim 4 *$\forall v_i \in \mathcal{C}, v_i \subset Vor(\mathcal{S})$.*

Proof. As $\epsilon_v \to 0$, $N(v_i) \subset S_i$. □

Claim 5 *$\forall e_{ij} \in \mathcal{C}, \{m_{ij}\} \cup \{\overline{v_i m_{ij}}, \overline{v_j m_{ij}}\} \subset Vor(\mathcal{S})$.*

Proof. WLOG take $x \in (v_i, v_j)$ such that $v_i \in N_0(x)$. As $\epsilon_v \to 0$, $N(x) \subset C_{ij}$, so x lies on a Voronoi edge. As $\epsilon_v \to 0$, $N(m_{ij}) \subset C_{ij} \cup C_{ji}$ so m_{ij} is a vertex. □

For $\triangle_{ijk}$, let β_i be the first intersection of the ray starting at v_i and bisecting its angle with any of $\{\overline{c_{ijk} m_{ij}}, \overline{c_{ijk} m_{ik}}, \overline{c_{ijk} m_{jk}}\}$.

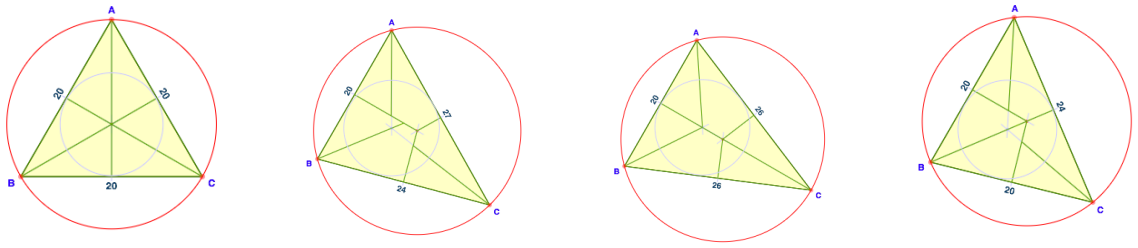

(a) $|AB| = |BC| = |AC|$. (b) $|AB| < |BC| < |AC|$. (c) $|AB| < |BC| = |AC|$. (d) $|AB| = |BC| < |AC|$.

Figure 1: Case analysis for refining a triangle into six facets, triangles and quads, based on the relative length of $\overline{AB}$. Voronoi edges (thick) lie on angle and edge-perpendicular bisectors (thin). Many edges are collinear.

Claim 6 $\forall \triangle_{ijk} \in \mathcal{C}$, *we have* $\{c_{ijk}, \beta_i, \beta_j, \beta_k\} \cup \{\overline{c_{ijk}m_{ij}}, \overline{c_{ijk}m_{ik}}, \overline{c_{ijk}m_{jk}}, \overline{v_i\beta_i}, \overline{v_j\beta_j}, \overline{v_k\beta_k}\} \subset \mathit{Vor}(\mathcal{S})$.

Proof. As $\epsilon_v \to 0$, $N(c_{ijk}) \subset S_i \cup S_j \cup S_k$. WLOG taking $x \in (c_{ijk}, m_{ij})$, $N(x) \subset C_{ij} \cup C_{ji} \cup C_{ik} \cup C_{jk}$ as $\epsilon_v \to 0$ so $\overline{c_{ijk}m_{ij}}$ is covered by a sequence of collinear Voronoi edges. Similarly, as $\epsilon_v \to 0$, $N(\beta_i) \subset C_{ij} \cup C_{ji} \cup C_{ik} \cup C_{jk}$ and taking $x \in (v_i, \beta_i)$, $N(x) \in C_{ij} \cup C_{ik}$ so $\overline{v_i\beta_i}$ appears exactly in $\mathrm{Vor}(\mathcal{S})$.

Let β_i' and β_j' be the intersections between the line supporting $\overline{c_{ijk}m_{ij}}$ and the rays bisecting the angles at v_i and v_j, respectively. We define an ordering on $\overrightarrow{m_{ij}c_{ijk}}$ such that $x_1 < x_2$ if $\|m_{ij} - x\| < \|m_{ij} - x_2\|$. WLOG, let $\beta_i' \leq \beta_j'$. We have the following cases; see Figure 1.

case	$\lvert\{e\}\rvert$	case	$\lvert\{e\}\rvert$
$\beta_i' = \beta_j' = c_{ijk}$	1	$\beta_i' < c_{ijk} < \beta_j'$	2
$\beta_i' < \beta_j' = c_{ijk}$	2	$c_{ijk} = \beta_i' < \beta_j'$	1
$\beta_i' = \beta_j' < c_{ijk}$	2	$c_{ijk} < \beta_i' = \beta_j'$	1
$\beta_i' < \beta_j' < c_{ijk}$	3	$c_{ijk} < \beta_i' < \beta_j'$	1

□

Claim 7 *Each* $\triangle_{ijk} \in \mathcal{C}$ *appears as 6 facets in* $\mathit{Vor}(\mathcal{S})$.

Proof. $\forall x \in \triangle_{ijk}$, $N(x) \subset C_{ij} \cup C_{ji} \cup C_{jk} \cup C_{kj} \cup C_{ik} \cup C_{ki}$. The mirrored pair of seeds on each of the six circles contributes a Voronoi facet aligned with $\triangle_{ijk}$. □

Corollary 8 *Letting* v, e *and* f *be the number of vertices, edges and facets in* $\mathcal{C}$*, the basic placement strategy in 2.1 generates at most* $v + 3e + 4f$ *vertices, at most* $2e + 9f$ *edges and exactly* $6f$ *facets in* $\mathit{VoRef}(\mathcal{C})$.

Theorem 9 *Given a PLC* $\mathcal{C}$ *satisfying the closeness condition,* $\mathcal{C} = \mathit{VoRef}(\mathcal{C})$.

Proof. ($\mathcal{C} \subset \mathrm{VoRef}(\mathcal{C})$) Claims 4, 5 and 7 establish that all vertices, edges and facets of $\mathcal{C}$ belong to $\mathrm{Vor}(\mathcal{S})$. By examining the arguments made above, it is clear that $\forall x \in \mathcal{C}$, x lies on some face in $\mathrm{Vor}(\mathcal{S})$ common to the appropriate number of correctly labeled seeds in $\mathcal{S}$.

($\mathrm{VoRef}(\mathcal{C}) \subset \mathcal{C}$) Assume for contradiction that $\exists x \in \mathrm{VoRef}(\mathcal{C})$ such that $x \notin \mathcal{C}$. By definition of $\mathrm{VoRef}(\mathcal{C})$, x lies on some face in $\mathrm{Vor}(\mathcal{S})$ common to at least two seeds with matching labels. But, as $x \notin \mathcal{C}$, no seeds in $\mathcal{S}$ would be labeled to retain it. □

3 Placement under Closeness with Non-zero Radii

Recall that per 2.1, all seeds in $\mathcal{S}$ were labeled with the associated face to serve as witnesses upon recovering the PLC from $\mathrm{Vor}(\mathcal{S})$. When $\epsilon_v, \epsilon_e \to 0$, ball neighborhoods free of input vertices were sufficient. Using non-zero radii, the natural analog is to require witnessed neighborhoods free of bad seeds. In this section, we also assume $\mathcal{C}$ satisfies the closeness condition.

One way to think of the *witnessed neighborhood* for $\triangle_{ijk}$ is to take a clone of its ball neighborhood endowed with the vertex spheres $\{S_i, S_j, S_k\}$ with ϵ_v set initially to 0. Then, as ϵ_v and ϵ_e increase to a non-zero value, the vertex spheres grow while the cloned ball neighborhood starts to shrink as the spheres centered at any $x \in \triangle_{ijk}$ need only touch the nearest witness in $\mathcal{S}_{ijk}$ rather than the original vertices $\{v_i, v_j, v_k\}$. As $\mathcal{S}_f$ refines f, the witnessed neighborhood is the union of spheres centered at the vertices $v \subset \mathrm{VoRef}(f)$ with radius equal to $\kappa_f(v)$.

If a seed s was not given an appropriate label for some x, we say s is a *non-witness* for x. If a non-witness seed $s \in \mathcal{S}$ is closer to x than its witnesses, then $\mathrm{Vor}(\mathcal{S})$ fails to conform to $\mathcal{C}$. The following definition characterizes problematic placements for non-zero radii.

Definition 10 (Encroached Faces) *If a non-witness seed* $s \in \mathcal{S} \setminus \mathcal{S}_f$ *lies in the witnessed neighborhood of* f*, we say that* s encroaches *on* f.

3.1 Non-overlapping Radii

The basic strategy in 2.1 was described for sphere radii ϵ_v and circle radii ϵ_e approaching zero. Here we show these radii can be non-zero.

If $\mathcal{C}$ is a planar triangulation, the basic strategy does not create encroachments. The radius of S_i can be in the range $[0, \lambda_i)$ where $\lambda_i = min_{(i,j)\in\mathcal{C}}\|v_iv_j\|/2$. This ensures vertex balls do not overlap, and only the faces and edges incident on v_i intersect S_i. For finite radii edge circles, let α_i be the minimum angle at v_i, then C_{ij} can have a radius in the range $[0, r_i \sin\frac{\alpha_i}{2})$ for all edges $(i,j) \in \mathcal{C}$. Again, this ensures that edge circles do not intersect, and only triangles incident on an edge intersect its circles. Although for non-zero radii each face is not partitioned as nicely as in 2.3, Corollary 8 and Theorem 9 still hold.

If $\mathcal{C}$ is non-planar, it may contain non-incident elements that come arbitrarily close together. Denote the minimum distance between any two non-incident features by δ_v. Set all sphere radii to $\epsilon_v = \delta_v/3 > 0$ [7]. Recalling that seeds lie on spheres of radius ϵ_v around input vertices, define the *clearance* at a point x on some face $f \in \mathcal{C}$ as $cl(x) = \kappa_0(x) - \kappa_f(x)$. A sufficient condition for encroachment-free witnessed neighborhoods can be stated as $cl(x) \geq \epsilon_v \ \forall x \in f$. The basic strategy achieves this when $\epsilon_e \to 0$. For $\epsilon_e > 0$, we amend the strategy and allow a slightly smaller upper bound. Consider a shrunken ball neighborhood that only extends to the seeds generated on the spheres around the vertices of the face; call this the (ϵ_v, ϵ_e)-neighborhood of f. We add extra seeds to provide a safe lower bound on clearance.

Recall that all points e_{ij} are protected by seeds on $C_{ij} \cup C_{ji}$. We ensure a similar protection for all points on a triangles $\triangle_{ijk}$. Fixing S_i, consider the two great circles going through the pairs of seeds generated on C_{ij} and C_{ik} for e_{ij} and e_{ik}, respectively, and perpendicular to $\triangle_{ijk}$. Let h_i be the smaller of the heights of those seed pairs. We add extra seed pairs on S_i with uniform spacing between the two great circles at height h_i. The spacing is chosen to ensure $cl(x) \geq \min\{cl(m_{ij}), cl(m_{ik}), cl(m_{jk})\} \forall x$ in the interior of $\triangle_{ijk}$, and the number of extra seeds is finite as $\epsilon_e > 0$.

Fixing a face $f \in \mathcal{C}$ and a non-incident vertex v_i, let p be the closest point on S_i to the $(\epsilon_v, 0)$-neighborhood of f and note that $\forall x \in f$, $\|x - p\| \geq \kappa_0(x) - \epsilon_v$. For $\epsilon_e > 0$, the (ϵ_v, ϵ_e)-neighborhood might contain p and intersect S_i in a circle C_{if}. We show that any seeds on S_i lie outside C_{if} and do not encroach. Consider edge e_{ij} incident on v_i with witnesses on C_{ij}. We have two cases: (1) $p \in e_{ij}$. As the radius of C_{if} is at most ϵ_e, C_{ij} lies outside the (ϵ_v, ϵ_e)-neighborhood. (2) $p \notin e_{ij}$. Let p' be the closest point of f's (ϵ_v, ϵ_e)-neighborhood to p, and let $q = S_i \cap e_{ij}$. Define δ_e as the minimum $\|p' - q\|$ for any such points p, q. Then, we require $\epsilon_e \leq \delta_e/3$. To account for edges incident on the same vertex, let α_{min} be the minimum angle between two incident features of $\mathcal{C}$ and define $\alpha^* = \min\{\alpha_{min}, \pi/10\}$. We set $\epsilon_e = \min\{\delta_e/3, \epsilon_v \cdot \sin(\alpha^*/3)\} > 0$.

The preceding discussion establishes the following statement.

Theorem 11 *Any PLC satisfying the closeness condition admits a finite refinement for some $\epsilon_v, \epsilon_e > 0$. If the PLC is planar, the refinement has linear size.*

Note that while δ_v is an intrinsic feature of the input PLC, δ_e apparently arises due to this specific approach. To yield larger δ_e, one may attempt refinement to further reduce ball neighborhoods, e.g., by regular subdivision. It would be interesting to enable larger non-zero radii that only depend on intrinsic input properties and derive a bound on the output size.

3.2 Fewer Steiner Points in 2D by Overlapping Radii

The primitives in 2.1 created non-overlapping vertex spheres and edge circles, and introduced many seeds on them. In particular, it generates twelve seeds for each triangle, with one pair for each half-edge. For adjacent edges around a vertex, if we can make edge circles larger so that they overlap, then we may use their two intersection points as the two necessary seeds for both edges, and generate only six seeds per triangle. Observe that the segment between such intersection points is perpendicular to the facet.

For vertices sharing an edge, if we make vertex spheres large enough to overlap, we may use the same seed pair for both endpoints of the edge, and again generate only six seeds per triangle. In the extreme, if we can perform both, this results in just one seed pair for all three edges of a triangle. We leave the study of these two additional variants as future work and only consider sharing seeds between edge circles around vertices.

Figure 2a shows schematically the basic setup for this scenario. For a given vertex v, we order the n edges in counter-clockwise order, and identify faces with the right edge. Let c_k denote the center of the circle for edge e_k and $\ell_k = \|v - c_k\|$. Each edge e_k gets two seed pairs that we denote by $s_1(k)$ (right) and $s_2(k)$ (left). If R is the radius of the sphere around vertex v, then the only restriction we have here is that $\ell_k < R \ \forall k$.

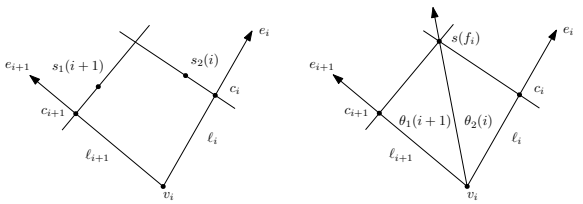

(a) Basic strategy: two seed pairs per vertex of a face.

(b) Overlapping circles: one seed pair shared by two edges.

Figure 2: Reducing the number of seeds per face.

We show how to use just three seed pairs per face by allowing circles of consecutive edges to share a pair. Figure 2b shows schematically the new situation. For a given vertex v, we now generate just one seed pair for each face f_i, denoted by $s(f_i)$ in the figure. By projecting that seed pair onto the face, $\overrightarrow{v\, s(f_i)}$ partitions the angle between e_i and e_{i+1} as $\theta_2(i)+\theta_1(i+1)$, where $\theta_1(k)$ and $\theta_2(k)$ denote the right and left angles around edge e_k. Observe that now $\{\ell_k\}$ are no longer independent.

$$\ell_{i+1} = \frac{\cos\theta_1(i+1)}{\cos\theta_2(i)} \cdot \ell_i. \tag{1}$$

WLOG, fixing ℓ_1 we find that:

$$\ell_1 = \Big(\frac{\cos\theta_1(1)}{\cos\theta_2(n)} \times \cdots \times \frac{\cos\theta_1(2)}{\cos\theta_2(1)}\Big)\ell_1. \tag{2}$$

Rearranging, we get the additional requirement that $\prod_{i=1}^{n} \frac{\cos\theta_1(i)}{\cos\theta_2(i)} = 1$.

One easy way to satisfy Equation 2 is to enforce that seed pairs are placed above and below angle bisectors. This immediately sets all ratios in the product to 1. However, letting γ_i denote $\|v - s(f_i)\|$, we need to ensure no prefix product results in some $\gamma_i > R$. Note that γ_i are related by a similar product of cosine ratios and that such products telescope. In particular, γ_{min} and γ_{max} correspond to θ_{min} and θ_{max}. Moreover, they are related by the following relation:

$$\gamma_{min} \cos\frac{\theta_{min}}{2} = \gamma_{max} \cos\frac{\theta_{max}}{2}. \tag{3}$$

If the triangulation is nonobtuse, we know that $\theta_{min} \leq \theta_{max} \leq \frac{\pi}{2}$ and the cosine is monotonically increasing. As we require $\gamma_{max} < R$, we can bound $\theta_{min} \geq 2\cos^{-1}\frac{R}{\sqrt{2}\gamma_{min}}$. An explicit bound is readily available if γ_{min} is expressed as a constant fraction of R. For example, requiring $\gamma_{min} \geq \frac{R}{2}$ yields $\theta_{min} \geq 17.87°$.

4 Refinement for Closeness

In the previous section, the closeness condition was essential to the the refinement strategies and analyses we presented. In this section, we show how to enforce such condition for an arbitrary input PLC.

4.1 Flat Complexes

We show that any PLC with *flat* dihedral angles can be refined, by showing that it can be refined into one satisfying the closeness condition. For clarity we will call the standard dihedral angle between two triangles sharing an edge the *edge-dihedral*. We define the *vertex-dihedral* for a triangle $\triangle_{123}$ and a vertex v_4 as the minimum edge-dihedral between $\triangle_{123}$ and one of the three triangles $\triangle_{124}, \triangle_{143}$, and $\triangle_{423}$. Obtuse edge- and vertex-dihedrals imply that v_4 lies outside S_{123}, the smallest enclosing sphere of $\triangle_{123}$.

Definition 12 (Flat Complex) *A PLC is* flat *if all edge- and vertex-dihedrals between* adjacent *faces are obtuse, where two faces are* adjacent *if they have a non-empty intersection.*

Lemma 13 *Any flat PLC can be refined into one with empty ball neighborhoods.*

Proof. First, refine to obtain nonobtuse triangles [4]. Second, iteratively refine every edge into two and every triangle into four through regular subdivision, stopping when all ball neighborhoods are empty. This will terminate because ball-neighborhoods shrink through subdivision, so eventually the only vertices v close enough to intersect a ball neighborhood of face f, are such that the original triangles containing v and f are the same or adjacent. Any such v on an adjacent face f' must lie outside the edge-diameter sphere of the common edge with f by the nonobtuseness of f'. Then, flatness ensures v lies outside the smallest enclosing sphere of f. □

Recall [1] that an ϵ-lfs sampling of a surface $\mathcal{M}$ is a set of points $\mathcal{P}$ on $\mathcal{M}$ such that $\forall x \in \mathcal{M}$, $\exists p \in \mathcal{P}$ such that $\|xp\| \leq \epsilon \cdot \mathrm{lfs}(x)$, where lfs denotes the *local feature size* defined as the distance from x to the *medial axis* of $\mathcal{M}$. It is well-known that a triangulation of an ϵ-lfs sampling, for a small enough ϵ, provides flat angles [1, 2]. Further, triangle edge lengths are small compared to the local feature size, so no regular subdivision in the proof of Lemma 13 is needed.

Theorem 14 *Any flat PLC can be refined. A nonobtuse triangulation with vertices from an ϵ-lfs sampling can be refined into a linear number of faces.*

4.2 Witness Refinement

We show that any PLC can be refined, even if dihedrals are not flat and the complex is non-manifold. The reason is that we can place *extra witness seeds* for each face, so they are the closest seeds for any face point. As before, seeds are mirrored pairs for triangles, and cocircular for edges. The method is analogous to nonobtuse triangle refinement [4], however we do not need to explicitly maintain a triangular cell complex.

Extra witness seeds. We split an encroached face with extra seeds, which shrinks its witnessed neighborhood. In general, if a seed s encroaches on a face f, then we split f near the point closest to s but outside any vertex sphere or original edge circle. For example, for a triangle with an adjacent edge making an acute vertex-dihedral, the seeds on the edge circle may encroach on the triangle. We split the triangle at the shared vertex's ball radius, mirrored through the triangle point closest to the edge; see Figure 3b.

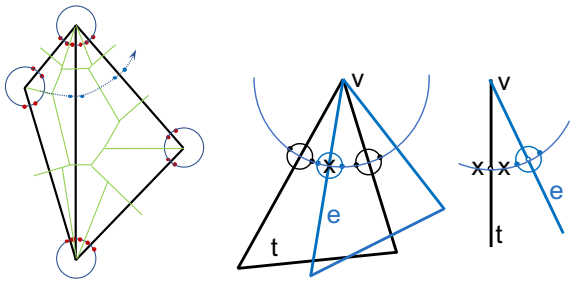

(a) Extra seeds (blue) splitting an edge opposite an obtuse edge-edge angle, and propagating.

(b) Top view (left) and side view (right), of triangle t and edge e with a sharp vertex-dihedral at v. Edge circle seeds encroach and induce a seed pair x on t.

Figure 3: Seed refinement on encroached faces. Edge-refinement would produce more Voronoi faces.

Note that the seeds introduced for a split may then encroach on a different face, which then requires further splits; see Figure 3a. We may have propagating paths, as in nonobtuse refinement [4], leading to splitting a face multiple times. Fortunately, there is a range of locations where a split will remove the encroachment. Limiting nonobtuse propagation paths is a lengthy analysis [4], and we leave a similar analysis for polynomial-size seed splitting of non-manifold complexes for future work.

However, we show that a finite refinement is achievable, by spacing seeds based on the geometry, with no propagation paths needed. Let all vertex balls have the same radius ϵ_v and all edge circles the same radius ϵ_e. Thus radii are non-zero but vertex spheres are non-overlapping, and edge circles are non-overlapping; see Section 3.1 for the details. For ease of exposition, let all subsequent extra seeds be infinitely close to the face they witness. Split all edges outside vertex balls into segments of length at most $\epsilon_e/2$. Form maximal packings of $\epsilon_t = \epsilon_e \sin(\alpha/2)/2$ radius spheres inside triangles, but outside the vertex spheres and ϵ_e-radius spheres around each split edge seed. Thus the closest seed to any face point is a witness seed. See Ebeida and Mitchell [6] for a similar construction.

Theorem 15 *Any PLC admits a finite refinement, including non-manifold triangulations.*

5 Conclusion

We showed how to generate a set of seed points such that the faces of the resulting Voronoi diagram conform to an arbitrary piecewise linear complex. The proposed seed placement strategies require certain neighborhoods to be empty of input vertices and can be ensured by a process similar to nonobtuse refinement of triangulations. The number of output faces depends on the complex's geometric and topological properties.

It would be interesting to generate an all-quadrilateral refinement. Without the optimizations, for scalene nonobtuse triangles the Voronoi faces are quadrilateral. The Voronoi cells that refine the input have "degenerate" position, being co-spherical and co-circular. It is unclear if this degeneracy allows further optimizations to reduce the number of Steiner points.

We leave open the problem of producing a polynomial bound on the number of seeds needed for non-planar triangulations. An analysis similar to Bishop [4] should suffice, but a path may cross an edge or triangle more times than in the planar triangulation case, and any polynomial bounds will likely be larger.

Acknowledgement

This material is based upon work supported by the U.S. Department of Energy, Office of Science, Office of Advanced Scientific Computing Research (ASCR), Applied Mathematics Program. Sandia National Laboratories is a multimission laboratory managed and operated by National Technology and Engineering Solutions of Sandia, LLC., a wholly owned subsidiary of Honeywell International, Inc., for the U.S. Department of Energy's National Nuclear Security Administration under contract DE-NA0003525.

References

[1] N. Amenta and M. Bern. Surface reconstruction by Voronoi filtering. *Discrete & Computational Geometry*, 22(4):481–504, Dec. 1999.

[2] N. Amenta and T. K. Dey. Normal variation for adaptive feature size. *CoRR*, abs/1408.0314, 2014.

[3] T. Biedl, M. Held, and S. Huber. Recognizing straight skeletons and Voronoi diagrams and reconstructing their input. In *10th International Symposium on Voronoi Diagrams in Science and Engineering*, 2013.

[4] C. J. Bishop. Nonobtuse triangulations of PSLGs. *Discrete & Computational Geometry*, 56(1):43–92, 2016.

[5] D. Engwirda. Conforming restricted delaunay mesh generation for piecewise smooth complexes. *Procedia Engineering*, 2016. 25th International Meshing Roundtable.

[6] M. S. Mohamed S. Ebeida and S. A. Mitchell. Uniform random Voronoi meshes. In *20th International Meshing Roundtable*, pages 258–275, 2011.

[7] M. Murphy, D. M. Mount, and C. W. Gable. A point-placement strategy for conforming Delaunay tetrahedralization. *International Journal of Computational Geometry & Applications*, 11(06), 2001.

[8] A. Rand and N. Walkington. Collars and intestines: Practical conforming Delaunay refinement. In *Proceedings of the 18th International Meshing Roundtable*, 2009.

[9] A. Spettl, T. Brereton, Q. Duan, T. Werz, C. E. Krill III, D. P. Kroese, and V. Schmidt. Fitting Laguerre tessellation approximations to tomographic image data. *Philosophical Magazine*, 96(2), 2016.